Modelling of auxetic networked polymers built from calix[4]arene building blocks

J. N. Grima[a]; J. J. Williams[b]; R. Gatt[a]; K. E. Evans[b]

[a] Department of Chemistry, University of Malta, Msida, MSD 05, Malta [b] Department of Engineering, University of Exeter, Exeter, EX4 4QF, UK

PLEASE SCROLL DOWN FOR ARTICLE

Modelling of auxetic networked polymers built from calix[4]arene building blocks

J. N. GRIMA†*, J. J. WILLIAMS†‡, R. GATT† and K. E. EVANS‡

†Department of Chemistry, University of Malta, Msida MSD 05, Malta
‡Department of Engineering, University of Exeter, Exeter EX4 4QF, UK

Auxetic materials (i.e. materials with a negative Poisson's ratio) expand laterally when stretched and become thinner when compressed. This unusual yet very useful property arises from the way by which the nano or microstructure of the material deforms when subjected to uniaxial mechanical loads. This paper discusses a novel class of molecular-level auxetic (networked polymers) built from calix[4]arene building blocks. These calix[4]arene subunits are connected in such a way that they mimic the shape of a "folded macrostructure" which is known to exhibit auxetic behaviour. We confirm through force-field based simulations that these newly proposed networked polymers exhibit negative Poisson's ratios, the magnitudes of which can be changed by introducing slight variations in the molecular structure of these polymers. We also develop simple geometry-based models which explain the values of the Poisson's ratios obtained through the force-field based simulations, and which give an insight into the features of the molecular structure that are responsible for the auxetic effect.

Keywords: Auxetic; Negative Poisson's ratios; Calix[4]arenes; Networked polymers

1. Introduction

Auxetic materials, i.e. materials with negative Poisson's ratios, exhibit the property of becoming wider when stretched and thinner when compressed [1], a property which contrasts with the behaviour of conventional materials that have a positive Poisson's ratios, (usually having a value of $0.25 \leq \nu \leq 0.33$) [2] and results in various improvements in the materials' macroscopic properties [3–5]. Although, at present it is unlikely that one encounters auxetic materials being used in everyday applications, research in this field has led to the discovery of negative Poisson's ratios in a wide range of man-made and naturally occurring materials such as man-made polymeric foams [4–9], nanostructured [1,10–12] liquid crystalline polymers [13,14] and microstructured polymers [15,16] and naturally occurring cubic metals [17], silicates [18–23] and zeolites [24–26].

In all of these systems, whether naturally occurring or man-made, the auxetic behaviour can be explained in terms of features in the materials' micro/nanostructure and the way the micro/nanostructure deforms when subjected to uniaxial stress. For example, the Poisson's ratios in the naturally occurring silicate α-cristobalite and in various zeolites have been explained using models where the molecular structure is described in terms of rigid units which, when loaded in tension rotate relative to each other to form a more open structure [23–26] whilst, the auxeticity in the liquid-crystalline polymers synthesised by Griffin *et al.* have been attributed to a model involving the rotation of laterally attached rods [13,14]. However, whilst naturally occurring materials have the obvious advantage that they need not be synthesised, man-made auxetics offer the advantage that their macroscopic properties may be controlled by modifying the synthesis or manufacture process and hence one may obtain materials which are designed to have a specific set of mechanical properties.

One approach for designing man-made molecular-level auxetics is to have a molecular structure that mimics the properties of another auxetic system, for example, a naturally occurring auxetic or an auxetic macrostructure. This can be achieved since the Poisson's ratio is a scale independent property, i.e. the Poisson's ratio is unaffected by the scale at which a particular "deformation mechanism" operates. In this respect, it should be noted

*Corresponding author. Email: joseph.grima@um.edu.mt www:http://home.un.edu.mt/auxetic

that if a geometry-based model for the behaviour of system is available, then this model could be used as a guide for fine-tuning the actual set of mechanical properties of the man-made auxetic.

This paper examines (through a force-field based molecular modelling study using the commercially available software package *Cerius*[2] (MSI Inc.) the potential for auxetic behaviour of various networked polymers built from calix[4]arene building blocks which are connected together through:

- a direct para–para connection (networked polymer 1a, see figure 1a);
- rod-shaped "rigid units" such as phenyl, or biphenyl units (networked polymers 1b–d, see figure 1b–d).

These systems, which we shall refer to as "double calixes" were chosen in an attempt to obtain systems that mimic the behaviour of a macrostructure which experimental testing has shown to exhibit negative Poisson's ratios [10]. This macrostructure (figure 2) is manufactured commercially from steel wire for use as an egg rack and is composed of alternate facing "four-legged claws" arranged on a square grid which when loaded in tension, opens up in all directions like an umbrella, hence producing a negative Poisson's ratio in the plane of the structure.

Geometry-based models which can relate the magnitudes of the Poisson's ratios as simulated by *Cerius*[2] to the molecular structure of the "double calix" networks will also be proposed in an attempt to obtain a better understanding of how these networks can be modified so as to obtain some particular set of mechanical properties.
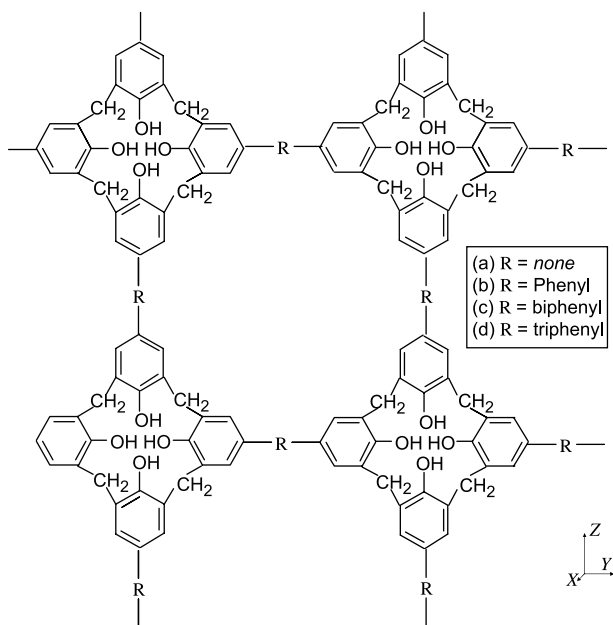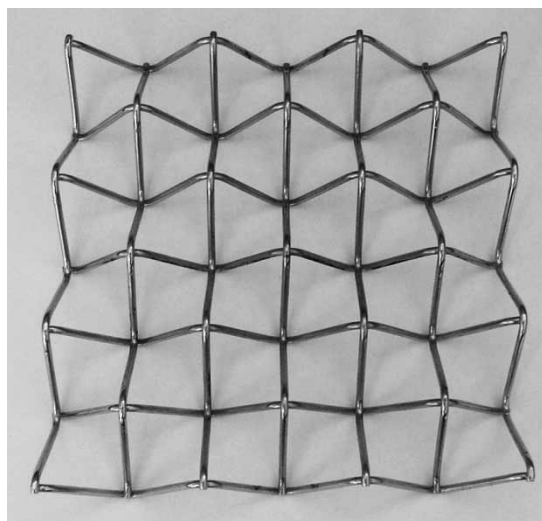

Figure 2. The auxetic macrostructure (30 × 30 cm) on which the molecular systems constructed here are based. This macrostructure is manufactured in steel and marketed as an 'egg rack'.

2. Identifying a suitable force-field for modelling calix[4]arenes: modelling of single calixes

Although a considerable amount of molecular modelling work has been performed on calix[4]arene systems [27–35], the suitability of force-fields available within *Cerius*[2] has not been assessed as yet. The choice of a force-field which correctly reproduces the properties of the systems to be modelled is crucial to the success or otherwise of the simulations (such as the ones on networked calixes presented in this paper) since in force-field based simulations, the quality of the results depend primarily on the suitability of the force-field in modelling the particular system. In this respect, the literature on modelling of calix[4]arene cones suggests that these systems are very sensitive to the force-field used. In particular, there have been some conflicting reports on the shape and symmetry that should be adopted by the cone conformer of tetrahydroxycalix[4]arenes. In particular, there were reports that the MM2 and early versions of the MM3 force-fields predict that the cone conformer with a C_{2v} symmetry is more stable than the C_{4v} by $2.5\,\mathrm{kJ\,mol}^{-1}$ ($0.6\,\mathrm{kcal\,mol}^{-1}$) [31–34]. This result was later shown to be an artefact of these force-fields which was "contrary to the general view that tetrahydroxycalix[4]arenes adopt a C_{4v} symmetric cone" [35]. In fact, direct evidence for the C_{4v} cone comes from experimental ^{1}H NMR and X-ray studies, where, for example, measurements with NMR spectroscopy have shown that tetrahydroxycalix[4]arenes adopt a C_{4v} geometry in various organic solvents [36,37], as well as in the gaseous phase [38] and in the solid state [39].

In view of this, we have simulated the minimum energies of single tetrahydroxycalix[4]arene molecules using four force-fields available within *Cerius*[2] Version 3.0 (Molecular Simulations Inc., San Diego, USA) which are parameterised to simulate the properties of organic

(a) R = *none*
(b) R = Phenyl
(c) R = biphenyl
(d) R = triphenyl

Figure 1. The molecular 'double calix' networks modelled.

systems namely the Dreiding 2.21 [40], Universal 1.02 [41], CVFF 950 [42] and PCFF 300 [43] force-fields. The atomic partial charges for use with the Dreiding and Universal force-fields were calculated using the charge equilibration procedure [44]. No cut-offs were used for the non-bond interactions. The minimum energy configurations were derived by minimising the potential energy as a function of the atomic coordinates using the SMART minimiser to the default $Cerius^2$ high convergence criteria (which include the criterion that the RMS force must be less than $0.001\,\mathrm{kcal\,mol^{-1}\,\mathring{A}^{-1}}$).

As illustrated in figure 3, these simulations show very clearly that only the PCFF 300 force-field correctly predicted the required C_{4v} symmetry for the tetrahydroxycalix[4]arene as the other three force-fields predicted a C_{2v} symmetry. The PCFF force-field also seems to predict the structure of tetrahydroxycalix[4]arenes fairy accurately as illustrated in table 1 in which structural properties as simulated by the various force-fields are compared to the equivalent properties obtained from X-ray crystallography data. Furthermore, the PCFF 300 force-field has been shown to correctly reproduce the order of stability for the Cone, Paco and 1,2-/1,3-Alternate conformers of tetrahydroxycalix[4]arenes, i.e. it correctly predicted that the cone conformer is more stable than the paco conformer, etc. [45].

All this suggests that the PCFF is a suitable force-field for simulating systems containing tetrahydroxycalix[4]arenes, and hence, this force-field will be the one used for all simulations on the networked systems.

3. Modelling of the networked systems

3.1 Methodology used in the simulations

Force-field based simulations were carried out on networks 1a–d (see figure 1) using the molecular modelling package $Cerius^2$ Version 3.0 (Molecular Simulations Inc., San Diego, USA). The networks were represented as crystalline systems where each unit cell contains four connected calix[4]arenes aligned in space as shown in figure 4, i.e. with the plane of the networks parallel to the *YZ* plane whilst in the third direction (i.e. the *X*-direction), the networks were allowed to stack freely "inside one another". Modelling simulations confirmed that this type of three dimensional stacking (where the calixes stack inside one another like egg racks, see

(a)   (b)

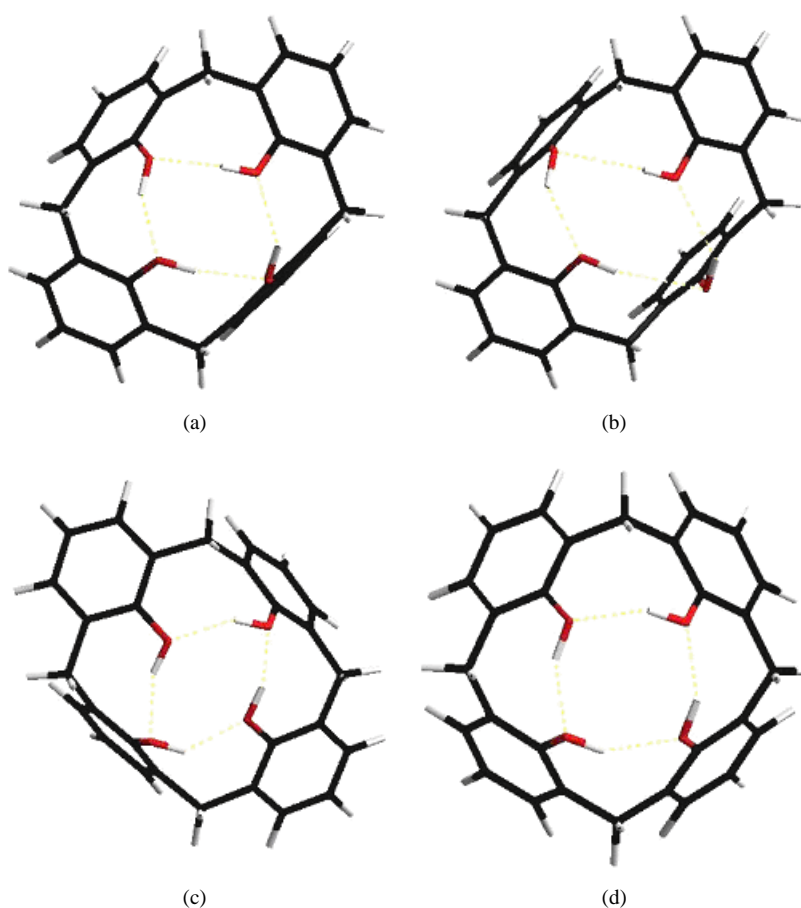(c)   (d)

Figure 3.   The minimised cone conformers of H calix[4]arene obtained using the (a) Dreiding; (b) Universal; (c) CVFF 950 and (d) PCFF 300 force-fields.

Table 1. Structural parameters of X-ray crystallographic and force-field optimized structures. (a) Dihedral angle (in degree) between each of the four phenyl rings in a calix, (Ph(A), Ph(B), Ph(C) and Ph(D)) and the 'mean plane' of bridging methylene carbons' ('methyl' plane); (b) Interatomic distance between neighbouring phenolic oxygen atoms on the four phenyl rings in a calix (Ph(A), Ph(B), Ph(C) and Ph(D)).

	X-ray data, taken from Shinkai and Harada, 1995 [37]	DRD	PCFF	CVFF	UFF
Torsion angle ϕ *(in degree)*					
[Ph (A)—'methyl' plane]	54.3	75.2	58.6	76.4	90.5
[Ph (B)—'methyl' plane]	54.3	41.6	58.6	30.1	37.0
[Ph (B)—'methyl' plane]	54.3	75.2	58.6	76.4	90.5
[Ph (D)—'methyl' plane]	54.3	41.6	58.6	30.1	37.0
Distance between two adjacent O atoms (in Å)					
O (A)—O (B)	2.65	5.757	2.769	2.720	3.069
O (B)—O (C)	2.66	2.841	2.769	2.733	3.394
O (C)—O (D)	2.65	2.757	2.769	2.720	3.069
O (D)—O (A)	2.65	2.841	2.769	2.733	3.394

figure 4) is the lowest energy (most stable) arrangement compared to other possible stacking arrangements such as for example where the calixes are "back to back" [45].

Energy expressions E for each of these five networks were set up using parameters from the PCFF 300 force-field where the non bond terms were added using the Ewald summation technique [46]. Energy minimisation was carried out to the default *Cerius*^{2} high convergence criteria. During the minimisation, all cell parameters were set as variables, i.e. no constraints on the shape or size of the unit cell were applied.

The mechanical properties of these single crystalline systems 1a–d were obtained by calculating the elements of the stiffness matrix $\mathbf{C} = [c_{ij}]$ from the second derivative of the minimised potential energy function since:

$$c_{ij} = \frac{1}{V}\frac{\partial^2 E}{\partial \varepsilon_i \partial \varepsilon_j} \quad i,j = 1,2,\ldots,6$$

where E is the energy expression, V is the volume of the unit cell and ε_i are strain components. This 6×6 stiffness matrix $\mathbf{C}$, and its inverse, the compliance matrix $\mathbf{S}$, relate

stress σ to strain ε as follows:

$$\sigma = \mathbf{C}\varepsilon \quad \text{or} \quad \varepsilon = \mathbf{S}\sigma = \mathbf{C}^{-1}\sigma$$

and can completely describe the mechanical properties of any anisotropic system.

4. Results and discussion

The simulations suggest that the minimum energy conformations of networks 1a–d possess a shape which is very similar to the "egg rack macrostructure" in that the "polyphenyl" chains (e.g. the biphenyl units in 1a where each phenyl ring comes from the adjacent calixes) assume a "straight" conformation, as expected, and are arranged in such a way that when viewed down the *x*-axes, they appear to have a rotational symmetry of order 4 (a direct consequence of the symmetry of the cones) with some deviations in the systems with longer poly-phenyl chains.

Furthermore, these simulations suggest that the minimum energy conformations of all systems minimise in such a way that the different layers stack in the third dimension in an arrangement which optimises the π–π interactions between phenyl rings in adjacent layers. In fact, the distance between parallel layers of calix[4]arenes in 1a was found to be 3.38 Å which is comparable to the distance between layers of graphite (3.35 Å) [47].

The on-axis mechanical properties (Young's moduli and Poisson's ratios) of systems 1a–d as simulated from the second derivative method are listed in table 2. These results suggest that all the networks exhibit negative Poisson's ratios in the plane of the networks (i.e. negative ν_{yz} and ν_{zy}) and positive Poisson's ratios in the other directions (i.e. ν_{xy}, ν_{yx}, ν_{xz} and ν_{zx}), in accordance with the properties of the "egg-rack" macrostructure on which these molecular networks are based.

However, in contrast with the behaviour of the idealised macrostructure which, as stated in table 1 exhibits Poisson's ratios of $\nu_{yz} = \nu_{zy} = -1$, these molecular-level systems have Poisson's ratios ν_{yz} and ν_{zy} which are less auxetic than the "target value" of -1, especially in the case of the smaller systems. These deviations from the
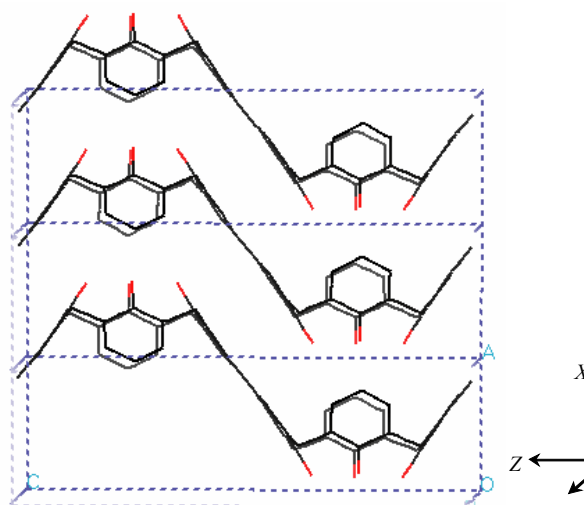

Figure 4. The three-dimensional structure of 1a as simulated by the PCFF force-field. Note the way this system is aligned in *XYZ* global axis system.

Table 2. The mechanical properties of the molecular systems 1a–d as simulated by the PCFF force-field compared to the properties of the 'egg rack' macrostructure.

	1a	*1b*	*1c*	*1d*	*Macroscopic 'egg rack' structure (idealised model)*
ν_{12}	0.36	0.52	0.63	0.70	+1
ν_{21}	1.42	1.18	1.07	1.16	+1
ν_{13}	0.36	0.52	0.64	0.69	+1
ν_{31}	1.42	1.18	1.03	1.17	+1
ν_{23}	−0.51	−0.87	−0.93	−0.95	−1
ν_{32}	−0.51	−0.85	−0.88	−0.96	−1
E_1 (GPa)	4.63	1.66	0.98	0.47	*n/a*
E_2 (GPa)	18.10	3.78	1.67	0.78	*n/a*
E_3 (GPa)	18.10	3.78	1.58	0.79	*n/a*

"target value (−1 is the only value)" as predicted by an analysis of the "egg rack macrostructure" can be explained if we consider a geometric model which represents the molecular network more accurately. For example, in a more accurate model, the joints in the structure should be replaced by "rhombuses" as shown in figure 5 in order to account for the fact that in the molecular systems, the four poly-phenyl chains making up one "umbrella" do not meet at a single point but "around a rim". The inclusion of these "rhombuses" has a significant effect on the properties of the system since whilst in the "original system" shown in figure 5a, loading in tension in the *Y* or *Z* direction will only cause an "opening" of the elements in an "umbrella-like fashion" (a process which will result in negative Poisson's ratios $\nu_{yz} = \nu_{zy} = -1$), loading of the "new structure" in figure 5b will result in deformations of the rhombuses (which would behave like the rhombic units in a "wine-rack", a process which would generate positive Poisson's ratios). These deformations occur concurrently to the auxetic "umbrella" mechanism, hence reducing the overall auxeticity of the system. Under such a description, the exact values of the Poisson's ratios will depend on: (i) the relative "rigidity of the rhombus" when compared to the "rigidity of the umbrellas" and (ii) the relative "size of the rhombus" when compared to the "size of the umbrellas". The latter effect can be demonstrated through the results of the simulations. These clearly suggest that the Poisson's ratios ν_{yz} and ν_{zy} tend to −1 as the number of phenyl rings between the calix[4]arenes increases (i.e. on going from 1a to d) as this increase causes the molecular

network to become more similar to the idealised "egg rack" (i.e. the "rhombus" become less prominent). However, it should be noted that as the networks become larger, the moduli decrease and hence the commercial applicability of these networks also decreases.

The simulations also suggest that the positive Poisson's ratios in *XY*- and *XZ*-planes (which in some cases assume very high values) are dependent on the length of the "polyphenyl chain". These Poisson's ratios are more difficult to interpret than the Poisson's ratios in the *YZ*-plane since the projection of the unit cell in the *X*-direction is dependent on the way that the different networked layers stack with respect to each other (there are no covalent bonds between these layers). In other words, we have a situation where, the networks are not physically connected but rather sit inside each other like empty egg cartoons (i.e. in register, see figures 3 and 6). The "opening" of networks in the *YZ*-plane due to tensile stresses in the *Y* or *Z* directions pushes adjacent layers into each other down the *X*-direction (a process which results in the positive ν_{yx} and ν_{zx}) whilst the pulling apart of the networks in the *X*-direction, due to tensile stresses in the *X* direction, causes closure of the calixes in the *YZ*-plane (a process which results in the positive ν_{xy} and ν_{xz}).

This behaviour may be explained through a simple geometry based model of the "stacking" where, referring to figure 6, as a first approximation we will assume that: (i) the separation *s* remains fixed in an attempt to optimise the $\pi-\pi$ interactions, and that (ii) the main mode of deformation is due to change in θ, i.e. θ is a variable but all other parameters are kept as constants. Although these assumptions may appear to be far-fetched, particularly, the assumption that *d* remains constant for loading in the *Z*-direction, they are supported by the PCFF molecular modelling simulations as shown in figure 7 which shows a superimposition of a "loaded" and "unloaded" system.
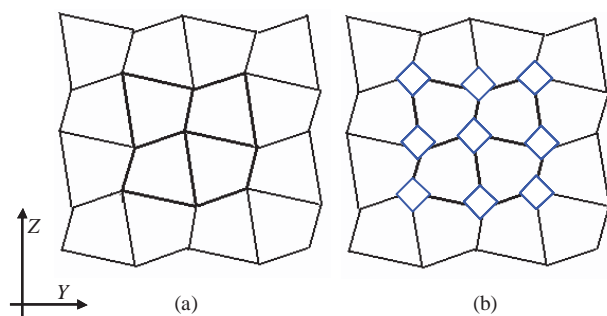

Figure 5. (a) The 'basic' idealised representation of these networks as 'connected umbrellas'; (b) a 'more accurate' representation which takes into consideration that fact that the poly-phenyl chains meet around a rim and not at a point.
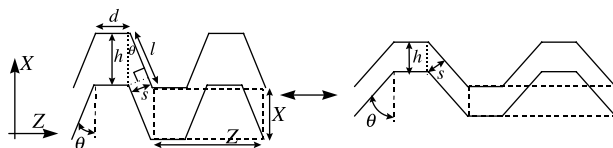

Figure 6. A geometric model for the behaviour of the system in the third dimension (i.e. in the *XZ*-plane, or its equivalent *YZ*-plane).
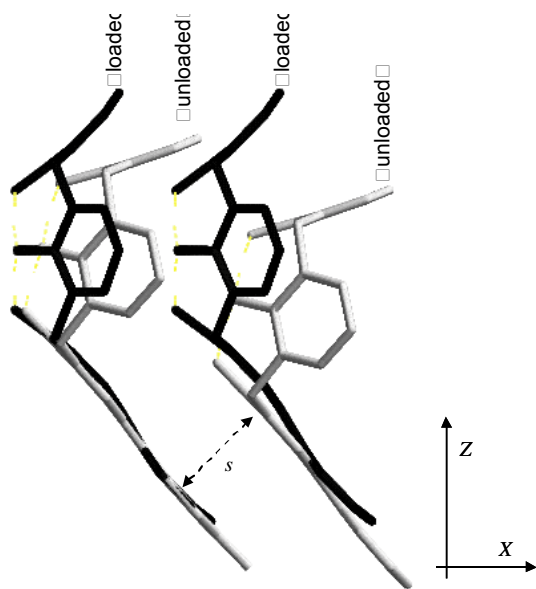
Figure 7. An overlay of a 'loaded' (shown in grey) and 'unloaded' (shown in black) form of system 1a as simulated by the PCFF force-field. (Loading in the *Z* direction). Referring to figure 6, note that loading in the *Z*-direction results in a significant change in the angle θ with only slight changes in *s*, *d* or *l*.

Under these assumptions, since the projection of the molecular networks in the *XZ*-plane (which from symmetry is equivalent to the *ZY*-plane) are given by:

$$X = h = \frac{s}{\sin(\theta)}$$

$$Z = 2[d + l\sin(\theta)]$$

the Poisson's ratios in the *XZ*-plane may be written as:

$$\nu_{zx} = \frac{1}{\nu_{xz}} = -\frac{d\varepsilon_x}{d\varepsilon_z} = -\left(\frac{1}{X}\frac{dX}{d\theta}\right)\left(\frac{1}{Z}\frac{dZ}{d\theta}\right)^{-1} = \ldots$$

$$= \frac{d}{l\sin(\theta)} + 1$$

This model suggests that for $0 < \theta < \pi/2$, since the term $d/l\sin(\theta)$ is positive, the Poisson's ratio ν_{zx} should assume values which are larger than $+1$ whilst ν_{xz} (which in this simple model is the reciprocal of ν_{zx}) is predicted to be between 0 and $+1$. The model also predicts that if *d* and θ are kept constant, the Poisson's ratios ν_{zx} and ν_{xz} tend to $+1$ as the magnitude of *l* increases (i.e. as the number of phenyl rings in the poly-phenyl chain increases on going from 1a to d) since the term $d/l\sin(\theta)$ becomes less significant. As illustrated in table 2, the trends in the values of Poisson's ratios as simulated by the PCFF force-field are in conformity with the predictions of this geometric model, hence suggesting that this simple geometric model provides a fairly good explanation for the behaviour of this system in the third direction.

5. General considerations and conclusions

Through this work we have shown that the systems made from calix[4]arenes have a potential to exhibit negative Poisson's ratios, and that we are able to explain the exact magnitudes of Poisson's ratios of these systems though geometry-based models. Furthermore, we have shown how the Poisson's ratios can be altered through very slight variations in the molecular structure, i.e. by varying the number of phenyl rings between adjacent calixes. This constitutes a very important step forward in the development of materials with negative Poisson's ratios and is of high commercial value since auxetics exhibit many enhancements in their macroscopic properties and are potentially superior to their conventional counterparts in many practical applications [3–5].

In this respect, it is important to note that these "double calix" systems could be particularly useful in applications involving the "trapping" of small molecules which are then released as the trapping material expands when stretched. The three-dimensional structure of the "double calixes" proposed here suggests that they have a natural disposition for trapping small molecules (single calixes have been extensively used for entrapment of small ions and molecules due to their cone shaped cavity [48–51]) as by being auxetic, these networks have the advantage over single calixes that the entrapped molecules could be released as and when needed by stretching the network in a uniaxial direction. Furthermore, since these networked calixes are layered structures, it likely that one may be able to control the rate of diffusion between layers simply by altering the internal distance between stacked calixes through stretching or compressing in the third direction.

All this is very significant as it highlights the many advantages that these systems have over most conventional materials. Given the recent advances in the chemistry of calix[4]arenes [51], we hope that this work will encourage further experimental research into these systems so as to enable the synthesis of the first purpose-built molecular level auxetic material.

Acknowledgements

References

[1] K.E. Evans, M.A. Nkansah, I.J. Hutchinson, S.C. Rogers. Molecular network design. *Nature*, **353**, 124 (1991).
[2] S.P. Timoshenko, J.N. Goodier. *Theory of Elasticity*, 3rd ed., McGraw-Hill, New York (1970).
[3] A. Alderson. A triumph of lateral thought. *Chem. Ind.*, **10**, 384 (1999).
[4] R.S. Lakes, K. Elms. Indentability of conventional and negative Poisson's ratio foams. *J. Compos. Mater.*, **27**, 1193 (1993).

[5] F. Scarpa, W.A. Bullough, P. Lumley. Trends in acoustic properties of iron particle seeded auxetic polyurethane foam. *P.I. Mech. Eng C–J. Mech. Eng. Sci.*, **218**, 241 (2004).

[6] R. Lakes. Foam structures with a negative Poisson's ratio. *Science*, **235**, 1038 (1987).

[7] K.E. Evans, M.A. Nkansah, I.J. Hutchinson. Auxetic foams-modeling negative Poisson's ratios. *Acta Metallorg. Mater.*, **42**, 1289 (1994).

[8] C.W. Smith, J.N. Grima, K.E. Evans. A novel mechanism for generating auxetic behaviour in reticulated foams: missing rib foam model. *Acta Mater.*, **48**, 4349 (2000).

[9] J.N. Grima, A. Alderson, K.E. Evans. An alternative explanation for the negative Poisson's ratio in auxetic foams. *J. Phys. Soc. Jpn*, **74**, 1341 (2005).

[10] J.N. Grima, J.J. Williams, K.E. Evans. Networked calix[4]arene polymers with unusual mechanical properties. *Chem. Commun.*, **32**, 4065 (2005).

[11] J.N. Grima, K.E. Evans. Self expanding molecular networks. *Chem. Commun.*, **16**, 1531 (2000).

[12] R.H. Baughman, D.S. Galvao. Crystalline networks with unusual predicted mechanical and thermal-properties. *Nature*, **365**, 735 (1993).

[13] C.B. He, P.W. Liu, A.C. Griffin. Toward negative Poisson ratio polymers through molecular design. *Macromolecules*, **31**, 3145 (1998).

[14] C.B. He, P.W. Liu, P.J. McMullan, A.C. Griffin. Toward molecular auxetics: main chain liquid crystalline polymers consisting of laterally attached *para*-quaterphenyls. *Phys. Status Solidi B*, **242**, 576 (2005).

[15] K.L. Alderson, K.E. Evans. Strain-dependent behaviour of microporous polyethylene with a negative Poisson ratio. *J. Mater. Sci.*, **28**, 4092 (1993).

[16] K.E. Evans, B.D. Caddock. Microporous materials with negative Poisson's ratios. 2. Mechanisms and interpretation. *J. Phys. D: Appl. Phys.*, **22**, 1877 (1989).

[17] R.H. Baughman, J.M. Shacklette, A.A. Zakhidov, S. Stafstrom. Negative Poisson's ratios as a common feature of cubic metals. *Nature*, **392**, 362 (1998).

[18] A. Yeganeh-Haeri, D.J. Weidner, J.B. Parise. Elasticity of alpha-cristobalite—a silicon dioxide with a negative Poisson's ratio. *Science*, **257**, 650 (1992).

[19] N.R. Keskar, J.R. Chelikowsky. Negative Poisson ratios in crystalline SiO_2 from 1st-principles calculations. *Nature*, **358**, 222 (1992).

[20] A. Alderson, K.L. Alderson, K.E. Evans, J.N. Grima, M. Williams. Modelling of negative Poisson's Ratio nanomaterials: deformation mechanisms, structure–property relationships and applications. *J. Metastable Nanocryst. Mater.*, **23**, 55 (2005).

[21] A. Alderson, K.E. Evans. Rotation and dilation deformation mechanisms for auxetic behaviour in the alpha-cristobalite tetrahedral framework structure. *Phys. Chem. Miner.*, **28**, 711 (2001).

[22] A. Alderson, K.L. Alderson, K.E. Evans, J.N. Grima, M.R. Willams, P.J. Davies. Modelling the deformation mechanisms, structure–property relationships and applications of auxetic nanomaterials. *Phys. Status Solidi B*, **242**, 499 (2005).

[23] J.N. Grima, R. Gatt, A. Alderson, K.E. Evans. On the origin of auxetic behaviour in the silicate α-cristobalite. *J. Mater. Chem.*, DOI: 10.1039/b508098c (2005).

[24] J.N. Grima, K.E. Evans. Auxetic behaviour from rotating squares. *J. Mater. Sci. Lett.*, **19**, 1563 (2000).

[25] J.N. Grima, R. Jackson, A. Alderson, K.E. Evans. Do zeolites have negative Poisson's ratios? *Adv. Mater.*, **12**, 1912 (2000).

[26] J.N. Grima, A. Alderson, K.E. Evans. Auxetic behaviour from rotating rigid units. *Phys. Status Solidi B*, **242**, 561 (2005).

[27] S. Simaan, S.E. Biali. Conformational analysis of calixarene derivatives substituted at the methylene bridges. *J. Phys. Organ. Chem.*, **17**, 752 (2004).

[28] P. Kane, D. Fayne, D. Diamond, S.E.J. Bell, M.A. McKervey. Modelling of the sodium complex of a calixarene tetraester in the 1,3-alternate conformation. *J. Mol. Model*, **4**, 259 (1998).

[29] S.E.J. Bell, M.A. McKervey, D. Fayne, P. Kane, D. Diamond. Molecular modeling of calixarenes with group I metal ions. *J. Mol. Model*, **4**, 44 (1998).

[30] P.D.J. Grootenhuis, P.A. Kollman, L.C. Groenen, D.N. Reinhoudt, G.J. Vanhummel, F. Ugozzoli, G.D. Andreetti. Computational study of the structural, energetical, and acid–base properties of calix[4]arenas. *J. Am. Chem. Soc.*, **112**, 4165 (1990).

[31] T. Harada, E. Rudzinski, S. Osawa, S. Shinkai. Computational studies of Calix(4)arene homologs: influence of 5,11,17,23- and 25,26,27,28-substituents on the relative stability of four conformers. *Tetrahedron*, **49**, 5941 (1993).

[32] T. Harada, F. Ohseto, S. Shinkai. Combined NMR-spectroscopy and molecular mechanics studies of oh-depleted calix[4]arenes—on the influence of OH groups on the relative stability of calix[4]arene conformers. *Tetrahedron*, **50**, 13377 (1994).

[33] T. Harada, S. Shinkai. Combined NMR-spectroscopy and molecular mechanics studies on the stable structures of calix[n] arenas. *J. Chem. Soc. Perkin Trans.*, **2**, 2231 (1995).

[34] F.L. Dickert, O. Schuster. Mass sensitive detection of solvent vapours with calix[n]arenes—conformational adaptation to the analyte. *Adv. Mater.*, **5**, 826 (1993).

[35] W.P. van Hoorn. Conformational and dynamical properties of Calixarenes. PhD Thesis, University of Twente, 1997.

[36] G. Happel, B. Mathiasch, H. Kämmerer. Preparation of some cyclo(oligo[(2-hydroxy-1,3-phenylene)methylene])s—spectroscopic analysis of their pseudorotation. *Makromol. Chem.*, **176**, 3317 (1975).

[37] C.D. Gutsche, J. Bauer. The conformational properties of calix[4]arenes, calix[6]arenes, calix[8]arenes, and oxacalixarenes. *J. Am. Chem. Soc.*, **107**, 6052 (1985).

[38] K.B. Lipkowitz, G. Pearl. Structural features of solid-state Calix(4)arene in the cone conformation. *J. Org. Chem.*, **58**, 6729 (1993).

[39] R. Ungaro, A. Pochini, G.D. Andreetti, V. Sangermano. The crystal and molecular-structure of calix[4]arene from phenol and its $(1-1)$ and $(3-1)$ acetone clathrates. *J. Chem. Soc. Perkin Trans.*, **2**, 1979 (1985).

[40] S. Mayo, S.B. Olafsaon, W.A. Goddard III. Dreiding—A generic force-field for molecular simulations. *J. Phys. Chem.*, **94**, 8897 (1990).

[41] A. Rappé, C. Casewit, K. Colwell, W.A. Goddard III, U.F.F. Skiff. A full periodic-table force-field for molecular mechanics and molecular-dynamics simulations. *J. Am. Chem. Soc.*, **114**, 10024 (1992).

[42] A. Hagler, E. Huler, S. Lifson. Energy functions for peptides and proteins. 1. Derivation of a consistent force-field including hydrogen-bond from amide crystals. *J. Am. Chem. Soc.*, **96**, 5319 (1974).

[43] H. Sun, S. Mumby, J. Maple, A. Hagler. An *ab initio* cff93 all-atom force-field for polycarbonates. *J. Am. Chem. Soc.*, **116**, 2978 (1994).

[44] A.K. Rappé, W.A. Goddard III. Charge equilibration for molecular-dynamics simulations. *J. Phys. Chem.*, **95**, 3358 (1991).

[45] J.J Williams, K.E. Evans, J.N. Grima. Modelling of calix[4]arene systems with unusual mechanical properties. Paper presented at the 2nd National Chemistry Symposium, Malta, 30th March 2004.

[46] N. Karasawa, E.A. Goddard. Acceleration of convergence for lattice sums. *J. Phys. Chem.*, **93**, 7320 (1989).

[47] A. Hunter, J. Singh, J. Thornton. *pi–pi*-interactions—Yhe geometry and energetics of phenylalanine phenylalanine interactions in proteins. *J. Mol. Biol.*, **218**, 837 (1991).

[48] D.J. Cram, J.M. Cram. Container Molecules and Their Guests, Monographs in Supramolecular Chemistry, Royal Society of Chemistry, Cambridge (1994).

[49] C.D. Gutsche. *Calixarenes, Monographs in Supramolecular Chemistry*, Royal Society of Chemistry, Cambridge (1989).

[50] J. Vicens, V. Böhmer (Eds.). *Calixarenes, A Versatile Class of Macrocyclic Compounds*, p. 280, Kluwer Academic Publishers, Dordrecht (1991).

[51] C.D. Gutsche. *Calixarenes Revisited, Monographs in Supramolecular Chemistry*, Royal Society of Chemistry, Cambridge (1998).